

1 Original Research Article

2 **Efficacy analysis of corneal crosslinking**
3 **(CXL): comparing epi-on and epi-off**
4 **procedures**

5

6

7

8

ABSTRACT

Purpose: To analyze the factors influencing the corneal crosslinking (CXL) efficacy and comparison of epi-on and epi-off procedures.

Study Design: modeling the efficacy of epi-off and epi-on CXL.

Place and Duration of Study: New Taipei City, Taiwan, between November, 2021 and December, 2021.

Methodology: Solving the rate equations for the CXL efficacy which includes the roles of concentration of the photosensitizer, riboflavin (RF), RF depletion effects, dynamic of light intensity, and the non-uniform distribution of RF in the stroma, or the diffusion depth of RF. Both steady-state and transient state features are explored for the efficacy, crosslink depth (CD) and the effects of epithelium layer for the epi-on situation.

Results: The steady-state efficacy is proportional to the square-root of [RF-concentration] / [light-intensity], The competing factors of reduced RF, $F(z)$, and reduced light intensity in the stroma determine the relative efficacy of epi-on and epi-off. For example, for $F(z) < 0.5$, epi-on is more efficient than epi-off. In contrast, in the transient state (with efficacy < 0.6), the efficacy is proportional to the light dose, and therefore epi-on is always less efficient than epi-off. The crosslink depth (CD) has an inverse trend, such that higher light intensity and lower RF concentration lead to deeper CD. The analytic formulas are developed under simplified conditions, in which numerical simulation is required for non-uniform distribution, and when RF depletion are included. Various strategies for improved steady-state efficacy and crosslink depth for epi-on CXL are explored including the use of higher RF concentration and lower light intensity; enhancing the RF diffusion by an electrode device, or diffusion enhancing medicine. The analytic formulas are compared with measured data.

Conclusion: For the steady-state epi-on is more efficient than epi-off, when the RF reduction factor is less than the light intensity gain factor. In contrast, in the transient state (with efficacy < 0.6), the efficacy is proportional to the light dose, and therefore epi-on is always less efficient than epi-off.

9 **Keywords:** corneal crosslinking; efficacy; photosensitizer; riboflavin; UV light.

10

11

12 **1. Introduction**

13 In 1998, Spoerl et al [1,2] proposed the use of UVA light (at 365 nm) and a
14 photosensitizer, riboflavin, for corneal collagen cross-linking (CXL) to increase the
15 corneal biomechanical strength and stabilize the ectatic cornea. The standard
16 Dresden (SD) protocol was proposed (in 2003) by Wollensak et al [3], in which a
17 UVA light intensity of 3.0 mW/cm^2 was applied to the cornea for an irradiation
18 time of 30 minutes, such that a light fluence (dose) of 5.4 J/cm^2 was delivered to
19 the cornea. To shorten the irradiation time of the SD protocol, accelerated CXL
20 was also developed [4,5], based on Bunsen and Roscoe law [6], leading to the AC
21 protocol given by light intensity of $I = (3,9,18,30,45) \text{ mW/cm}^2$, with the
22 associated irradiation time is inverse proportional to the light intensity given by
23 $t = (30,10,5,3,2)$ minutes, such that the total dose applied to the cornea is fixed
24 at 5.4 J/cm^2 [1].

25 The basic kinetics and modeling of CXL were published by various groups [6-
26 10] and, more recently, by Lin et al [11-25]. The review articles by Lin et al
27 [26,27] discussed the critical and controversial issues of CXL, including: (i)
28 validation of SD protocol for the minimum (safety) corneal thickness of 400 μm ;
29 (ii) validation of the Bunsen and Roscoe law (BRL) of reciprocity for accelerated
30 CXL protocol; (iii) the role of oxygen in type-I and type-II CXL; (iv) Improved
31 efficacy by pulsed light and by higher riboflavin concentration; (v) the new
32 efficacy scaling law developed by Lin, a nonlinear law replacing the linear law
33 based on BRL; (vi) New criteria for minimum corneal thickness, in which
34 sub400 μm thin corneas (214 - 398 μm) was reported by Hafez et al [28].

35 The present article will further explore the features of CXL with an
36 emphasis on the role of riboflavin concentration on the crosslink depth and the
37 demarcation line depth, the critical parameters defining the outcome efficacy of
38 CXL. We will also compare our formulas with the measured data [29,30]. Epi-on
39 offers many clinical advantages of less post-operation pains, faster epithelium
40 recovery and less haze. Therefore, strategy for improved the efficacy and
41 crosslink depth for epi-on CXL is clinically important. The efficacy CXL of steady-
42 state and transient-state are compared for epi-on and epi-off. Our formulas
43 show that epi-on has lower transient-state efficacy than epi-off, as
44 conventionally believed. However, opposite trend is found for the steady-state
45 efficacy, a new finding to be explored experimentally.

46

47 **2. Materials and Methods**

48 **2.1 Epi-off versus epi-on**

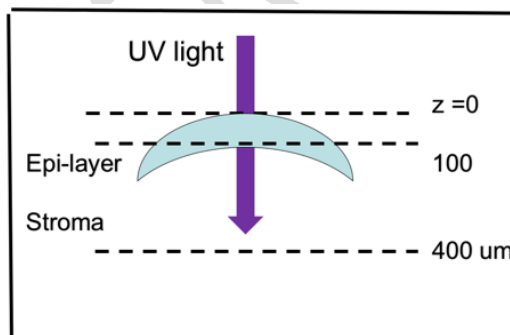
49 As shown in Fig. 1, a cornea under a UV light (at 365 nm), with epi-on
50 surface defined at $z=0$, and stroma thickness about 400 μm . The riboflavin
51 concentration distribution for epi-off (Curve-1) and epi-on (Curve-2), noting that
52 epi-off stroma surface defined by $z=100 \mu\text{m}$. Effect of RF distribution is
53 approximated by a distribution function $F(z)=1-0.5z/D$, or $C(z,t=0)=C_0F(z)$, with a

54 diffusion depth D in the stroma. We note that D is proportional to the waiting
 55 time of the pre-operation RF drops applying to the cornea. For a typical waiting
 56 time of 15 minutes (for epi-off), and 25 minutes (for epi-on), D is about $150\ \mu\text{m}$
 57 [12]. For example, for $C(z=0)=0.2\%$, at $z=300\ \mu\text{m}$, $C(z)=0.12\%$ and 0.08% for epi-
 58 off and epi-on, respectively, in which $C(z, \text{epi-on})$ is about 65% of epi-off. We will
 59 show later that lower $C(z)$ leads to lower efficacy.

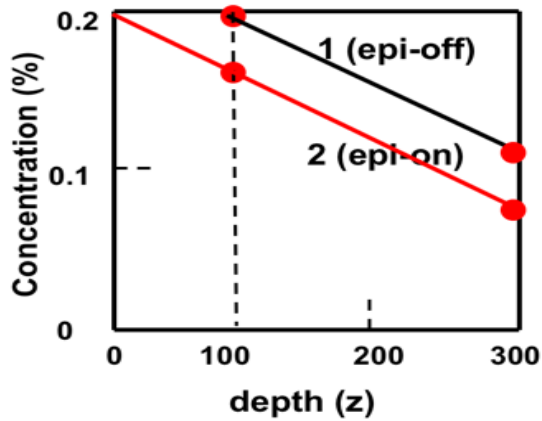
60 The light intensity is given by $I(z,t)=I_0 \exp(-q'z)$, with the effective absorption
 61 constant given by [22] $q'=2.3(a'C_0+Q)(1-Bt)$, with $B=1.15C_0(a'-b')d'$, d' is the
 62 correction for a depleted $C(t)=C_0 \exp(-d't)$; and $a'=204\ (\text{1/5 cm})$, $b'=120\ (\text{1/\% cm})$,
 63 and $Q=13.9\ \text{cm}^{-1}$; are the extinction coefficients of RF and the photolysis
 64 product, and stroma, respectively. Given a value of $q'=0.0094\ (\text{1/}\mu\text{m})$, with
 65 neglected $B=0$, we calculate the light intensity reduction factor (R') due the epi-
 66 layer (having a thickness of $Z_0=70$ to $100\ \mu\text{m}$), $R'=\exp(-q'Z_0)=0.4$ to 0.56 .
 67 Therefore, the reduced light intensity leads to a higher steady-state efficacy (to
 68 be shown later). Our formulas are consistent with the clinical studies of Lang et
 69 al [5] showing that accelerated CXL (ACX) had less efficacy than standard low
 70 intensity (3mW/cm^2) CXL for the same fluence (dose).

71 Combining the difference of D -value at $z=300\mu\text{m}$, $D(\text{epi-on})=0.65 D(\text{epi-}$
 72 $\text{off})$, we obtain the effective-ratio (of epi-on and epi-off), $ER=C_0/I_0=1.16$ to 1.63 .
 73 This ER is a critical parameter defining efficacy and crosslinking depth (to be
 74 discussed later). We note that (to be shown later) due to the special feature of
 75 CXL steady-state efficacy is governed (proportional to)
 76 $ER^{0.5}=[F(z)C_0/I_0]^{0.5}\exp[0.5q'(z+Z_0)]$. Therefore, the competing factors of $F(z)$ and
 77 $\exp(0.5q'Z_0)$ determines the relative efficacy of epi-on and epi-off. Our theory
 78 will predict that, under certain conditions, epi-on has a higher steady-state
 79 efficacy than that of epi-off, a feature in contrary to conventional concept, which
 80 is valid only for transient efficacy which is proportional to the light dose, or
 81 intensity x irradiation time (t), $E_0= tI_0$.

82
83



84
85 Fig. 1. Cornea under a UV light crosslinking, with (epi-on) surface defined at $z=0$, and
86 stroma thickness about $400\ \mu\text{m}$.
87



88 Fig. 2. Riboflavin concentration distribution for epi-off (Curve-1) and epi-on (Curve-
 89 2), noting that epi-off stroma surface defined by $z=100 \mu\text{m}$.
 90
 91

92

93

2.2 Crosslink Rate Equation

94 Using the shorthand concentration notations: C and T for RF ground and
 95 excited triplet state; R for the active radical, S for the singlet oxygen; and [A] for
 96 the available extracellular matrix substrate, the crosslinking rate equation is
 97 given by [22, 23, 26]

$$98 \quad \frac{d[A]}{dt} = -(K_3T + K_1R + K_2S)[A] \quad (1)$$

99 Eq. (1) includes three crosslink pathways: (i) the type-I direct coupling of T and
 100 the substrate [A]; (ii) and the coupling of the radical (R) and [A]; and (iii) the
 101 oxygen-mediated, type-II term due to the singlet oxygen coupling with [A]. Both
 102 type-I and type-II pathway can occur simultaneously, and the ratio between
 103 these processes depends on the type of photosensitizers (PS) used, the
 104 concentrations of PS, substrate and oxygen, the kinetic rates involved in the
 105 process, and the light intensity, dose, RF depletion rate etc.

106 In the type I mechanism, by receiving energy from UV light, RF becomes the
 107 excited RF triplet (T^*), which interacts directly with the substrate (i.e., stromal
 108 proteins). In the type II mechanism, T^* reacts with oxygen dissolved in stroma to
 109 produce reactive oxygen species (ROS), including singlet oxygen, hydroxyl radical
 110 and hydrogen peroxide, which generate photo-oxidation and photo-
 111 polymerization of the substrate. Overall, the dominant pathway of type I or type
 112 II depends on the type and concentration of photosensitizer, concentrations of
 113 substrate and the amount of oxygen [27].

114 2.3 The Efficacy formulas

115 Factors influencing the CXL efficacy include: UV light intensity, dose,
 116 exposure time, mode of exposure (pulsed or CW), riboflavin concentration,
 117 diffusion and drops pre-operation and interoperation administration, the
 118 concentration of oxygen in the stromal tissue (pre-op and inter-op), and
 119 environmental conditions. The length of the riboflavin presoaking time and
 120 viscosity of the riboflavin film also affect the crosslink depth. We will first
 121 consider the uniform RF distribution in the stroma, given by a distribution
 122 function $F(z)=1-0.5z/D$, with $D \gg 500 \mu\text{m}$, or $F(z)=1$. Therefore, the z-dependence
 123 of $C(z,t)$ is mainly due to light absorption. The effects of D (with D about 150 to
 124 $200 \mu\text{m}$) will be discussed later, in section 2.4.

125 For type-I dominant case, from Eq. (1), with $K_2S=0$, and for bimolecular
 126 termination dominant, we obtain, $R=(K_3[A]T/k')^{0.5}$, with $T=bl(z)gC(z,t)$. For g is
 127 approximated as $g=1/(K_3[A])$, R becomes $R=(T'/k')^{0.5}$, with $T'=bl(z)C(t)$, we obtain
 128 [26] (at a given z)

$$129 \frac{d[A]}{dt} = -T' + K_1 \sqrt{T'/k'} [A] \quad (2)$$

130 Considering a non-perfect RF regeneration case with $C(t)=C_0 \exp(-d't)$, with
 131 $d'=blg''$, and g'' defining the degree of regeneration (with $g''=0$, for the perfect
 132 case). the approximated analytic solution of Eq. (2) leads to the crosslink efficacy
 133 (CE) defined by $CE=1-[A]/[A_0]$,

$$134 CE = 1 - (1 + k H') \exp(-H) \quad (3)$$

135 where $k=bl(z)C_0(z)/A_0$ is the contribution from the K_3T term; $H(t)=2d[1-\exp(-$
 136 $0.5d't)]/d'$, $H'(t) = [1-\exp(-0.5d''t)]/d''$, with $d=K_1(blC_0/k')^{0.5}$, $d'=blg''$ and $d''=d'-$
 137 $0.5d$. Eq. (3) has transient state, $H(t)=dt$, $H'=0.5d''t$. The steady state $H=2d/d'=$
 138 $K_1[C_0/(bkg'l)]^{0.5}$, and $H'(t)=1/d''$, which is proportional to $(C_0/l)^{0.5}$, an increasing
 139 function of C_0 , but decreasing function of the light intensity, $I(z)=I_0 \exp(-A'z)$.
 140 Therefore, higher light intensity leads to lower steady-state efficacy. In contrast,
 141 the transient state $H=dt$, leading to efficacy proportional to $t(I_0C_0)^{0.5}$ or $(tE_0C_0)^{0.5}$,
 142 which is proportional to the light dose and irradiation time (t). These scaling laws
 143 having opposite power dependence of light intensity are also demonstrated
 144 numerically [15]. The special feature of steady-state efficacy is due to the RF
 145 concentration depletion which is proportional to light intensity, or $C(t)=C_0 \exp(-$
 146 $dt)$, with $d=K_1(blC_0/k')^{0.5}$, and the CXL radical is proportional to $(T'/k')^{0.5}$, with
 147 $T'=bl(z,t)C(t)$, in which the time integral of $R(z,t)$ defines the CXL efficacy, as
 148 shown the rate eq. (2).

149 **2.4 Crosslink-Depth (CD) and Demarcation line depth (DLD)**

150 CD and DLD are proportionally related, because both are defined by when
 151 CE is larger than an efficacy threshold value (E') for collagen tissue to be

152 effectively crosslinked, where E' may be different for CD and DLD. For type-I of
 153 Eq. (3), the steady state $H=2d/d'=2K_1[C_0/(bgk'l_0)]^{0.5}$, with $I(z)=I_0 \exp(-q'z)$; and let
 154 $CE=E'$ (for $H'=0$), or $H=\ln[1/(1-E')]=\ln E''$, we obtain (for type-I) DC (and DLD) are
 155 given by, assuming a uniform distribution, with $F(z)=1$, or diffusion depth
 156 $D \gg 500 \mu\text{m}$, and redefining $Z'=0$ at stroma surface (for epi-off case)

$$157$$

$$158 \quad Z' = (2/q') \ln(\ln E''/G) \quad (4.a)$$

159
 160 with $G=K_1[C_0/(bgk'l_0)]^{0.5}$; $q'=2.3(a'C_0+Q)(1-Bt)$, with $B=1.15C_0(a'-b')d'$, $K=2K'l_0^{-0.5}$,
 161 and $E''=1/(1-E')$; d' is the correction for a depleted $C(t)=C_0 \exp(-d't)$. Given a value
 162 of $q'=0.01$ ($1/\mu\text{m}$), with neglected $B=0$, and let $G'=\ln E''(bgk')^{0.5}/K_1$, Eq. (4.a)
 163 becomes

$$164$$

$$165 \quad Z' = 200 \ln(G' \sqrt{I_0/C_0}) \quad (4.b)$$

166
 167 for I_0 in mW/cm^2 and Z' in μm . We note that Z' is an increasing function of
 168 $[C_0/I_0]^{0.5}$ and $\ln(E'')$.

169

170 2.5 Effect of diffusion depth (D)

171 In the above formulas, we assume a uniform RF distribution in the stroma. A
 172 more realistic modeling was also developed by Lin et al [15] to include the effect
 173 of RF distribution. given by a distribution function $F(z)=1-0.5z/D$, or
 174 $C(z,t=0)=C_0F(z)$, with a diffusion depth D in the stroma. Another factor is the light
 175 absorption due the epithelium layer (of epi-on case). Comparing to epi-off, the
 176 revised light intensity for epi-on is reduced by a factor of $\exp(-q'z'')$, with z'' being
 177 the epi-layer (about 70 to 100 μm , mean of 80 μm , or 0.008 cm). Thus the
 178 effective absorption is revised to $q'=0.008+2.3(a'C_0+Q)(1-Bt)$, with $B=1.15C_0(a'-$
 179 $b')d'$ and d' is about 150 (1/sec), for $I_0=30 \text{ mW}/\text{cm}^2$. For RF (and with $C_0=0.2\%$,
 180 $B=0$), $a'=204$ ($\%.\text{cm}^{-1}$), $b'=120$ ($\%.\text{cm}^{-1}$) and $Q=13.9$ (1/cm) [15],
 181 $q'=0.008+0.0094=0.017$ (for epi-on); and $q'=0.0094$ (for epi-off). To include the
 182 light intensity dynamics, we revise $I(z,t)=I_0 \exp(+Bzt)$, thus Eq. (4.a) becomes,

$$183$$

$$184 \quad Z' = \ln(G' \sqrt{I_0/C_0}) / [q'(1 - 0.5/(q'D))] \quad (5)$$

185
 186 where $q'=0.0094$ (for epi-off), and 0.017 (for epi-on) which is 1.8 times larger.
 187 Therefore, to compensate the reduced CD in epi-on, we propose: (i) increase of
 188 light intensity (I_0) by a factor of 36, because $\ln 6=1.8$, to achieve the same Z' ; (ii)
 189 using a 36 times lower C_0 ; (iii) using 10 times higher I_0 and 3.6 lower C_0 ; and (iv)
 190 enhancing the RF diffusion (or larger D value) by an electrode device, or
 191 diffusion enhancing medicine. We note that the above means for increased CD is
 192 opposite to that of efficacy, to be discussed later.

193

194 1. Results and Discussion

195 3.1 The role of RF concentration

196 Lombardo et al [30] disclosed an apparatus to measure the intrastromal
 197 riboflavin concentration of the cornea and provides biomarkers of treatment
 198 efficacy in real time. The differences between samples could be primarily caused
 199 by: (i) frequency application of riboflavin drops pre-op and intra-op, (ii) non-
 200 uniform distribution of riboflavin film over the stromal surface, and (iii)
 201 distribution of riboflavin in the stroma. The exponential decrease of intrastromal
 202 riboflavin concentration during UV illumination is due to the consumption of
 203 riboflavin in the stroma, which is also temporally monotonic decreasing. Their
 204 results were fit to an exponential law, $C(t) = C_0 \exp(-t/\tau)$, with C_0 being the initial
 205 value and intrastromal riboflavin consumption rate $1/\tau$, with $\tau=12.8$ minutes, fro
 206 light intensity of 3 mW/cm^2 , in which the mean consumption of riboflavin was
 207 $80\pm 4\%$. During UV-A irradiation, the stromal riboflavin concentration decreased
 208 non-linearly. O'Brart et al [29] reported that efficacy is an increasing function of
 209 RF concentration (in the stroma).

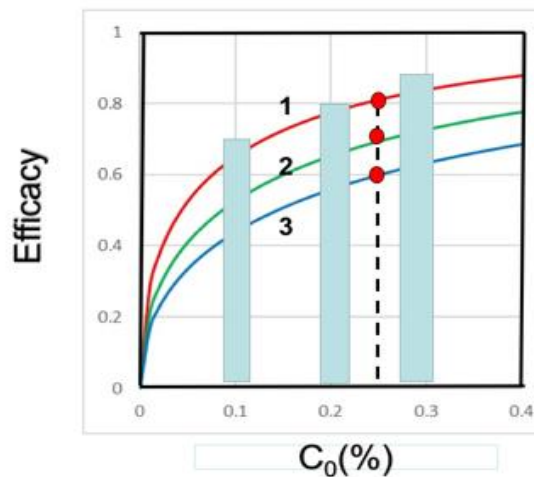
210 Clinical studies of Lang et al [5] showed that accelerated CXL (ACX) had less
 211 efficacy than standard low intensity (3mW/cm^2) CXL for the same fluence (dose)
 212 based on BRL. To overcome this intrinsic drawback of ACX, Lin [20] recently
 213 proposed a new protocol called the riboflavin concentration controlled method
 214 (CCM) to improve the efficacy of ACX by supplemental RF during the UV
 215 exposure to compensate for fast depletion of RF by UV light. However, RF
 216 concentration, $C(t)$, may be partially self-compensated due to the regeneration
 217 effect (RGE), in which $C(t) = C(z,t) = C_0 \exp(-bg''t) = C_0$, for a perfect RGE case with
 218 $g''=0$, which also depends on the type of photoinitiator [26]. The optimal
 219 concentration was also theoretically proposed [23], specially for the efficacy in
 220 the stroma (with $z>0$. From Eq. (4), the type-I steady-state efficacy given by $H =$
 221 $2K_1[C_0/(bgk'l)]^{0.5}$, which is an increasing function of $[C_0/I_0]^{0.5}$.

222 As discussed in our previous paper [22], $C(t)$ is a constant if there is a
 223 continuing resupply of RF, or for the case of a perfect REG of RF (or a catalytic
 224 cycle). To demonstrate the RF depletion, we conducted a measurement of RF
 225 (mixed with pure water) under UV irradiation at various RF concentrations, in
 226 which the increase of light intensity passing through the RF solution (path of 10
 227 mm) was recorded indicating the decrease of RF which also has color changes.
 228 This feature can be explored by $I(z,t) = I_0 \exp[-q' + Bt]z$, a revised time-dependent
 229 Beer-Lambert law (BLL) [11,17], with $B = 2.3(a'-b')C_0d'$, proportional to the
 230 depletion rate of RF (d') and its initial concentration C_0 . If $d'=0$, then $I(t,z)$ is time-
 231 independent.

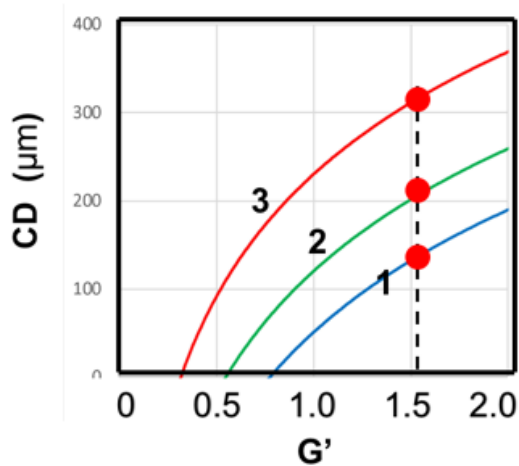
232 Fig. 3 shows the calculated efficacy, based on Eq. (3), versus RF
 233 concentration (C_0) at various light intensity; also shown are the measured data of
 234 O'Brart et al [41], in which efficacy is an increasing function of C_0 ; however, it is a
 235 decreasing function of the light intensity (for a given light dose). For examples,
 236 (shown by the red lots of Fig.1), efficacy $CE = (0.8, 0.7, 0.6)$, for $I = (9, 18, 30)$
 237 mW/cm^2 , at a given $C_0 = 0.25\%$. The measured data of O'Brart et al [41] are fit to
 238 our calculated curve.

239 Fig. 4 shows the calculated crosslink depth (CD) versus light intensity,
 240 based on Eq. (4.b), for various G' . We note that CD is an increasing function of

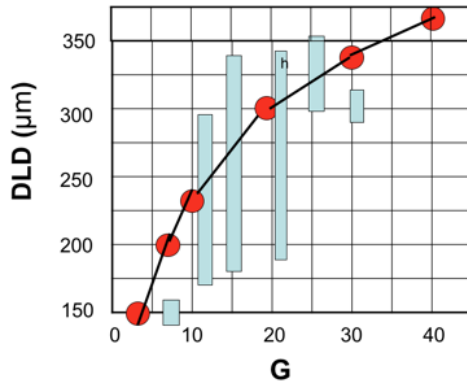
241 $(I_0/C_0)^{0.5}$ as shown by Eq. (4.b), which is proportional to the light intensity, but
 242 decreasing function of RF concentration, for steady-state efficacy. That is high
 243 concentration leads to a smaller CD. However, higher light intensity leads to
 244 deeper crosslink. These steady-state features are opposite to the transient state,
 245 in which CD is proportional to the light dose, $E_0=I_0 t_0$ and C_0 .
 246



247
 248 Fig. 3. Calculated efficacy versus RF concentration (C_0) at various light intensity $I=$
 249 (9,18,30) mW/cm^2 , for curves (1,2,3); also shown are the measured data of O'Brart
 250 et al [29], shown by blue bars.
 251



252
 253
 254 Fig. 4. Calculated crosslink depth (CD) versus G' for various light intensity, based on
 255 Eq. (4.b), for $C_0=0.25\%$, and various $I_0=(3, 48, 60) \text{mW}/\text{cm}^2$, for curves (1,2,3).



256
 257 Fig. 5. Demarcation line depth (DLD) versus threshold ratio factor G , for intensity $I=$
 258 10 mW/cm^2 , where bars are measured data of Hafez et al [29], and red dots are
 259 calculated, based on Eq. (4.b)

260 3.2 The competing factors in epi-on and epi-off

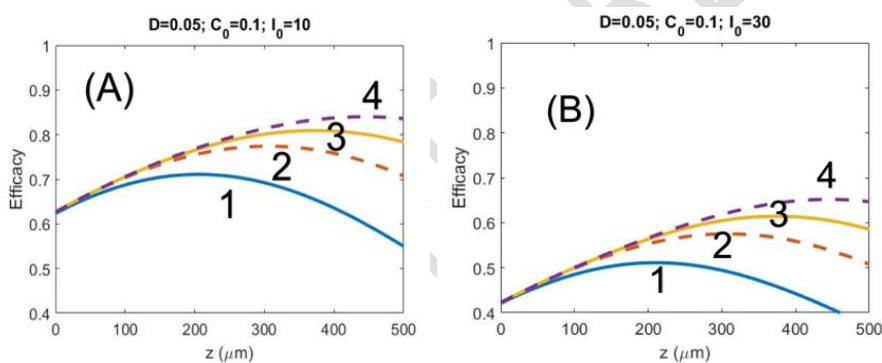
261 A more realistic modeling was also developed by Lin et al [15] to include the
 262 effect of RF distribution, given by a distribution function $F(z)=1-0.5z/D$, or
 263 $C(z,t=0)=C_0F(z)$, with a diffusion depth D in the stroma. We note that D is
 264 proportional to the waiting time of the pre-operation RF drops applying to the
 265 cornea. In this case CXL efficacy requires numerical simulation [15], with results
 266 shown in Fig. 6, in which the optimal efficacy is due to the competing effects of
 267 $F(z)$, a decreasing function of z , and the steady-state efficacy is proportional to
 268 $[F(z)C_0/I_0]^{-0.5}\exp(0.5q'z)$, having an increasing function of z , $\exp(0.5q'z)$.
 269 Mathematically this can be calculated by $dG(z)/dz=0$, to find the optimal z^* ,
 270 $G(z)=F(z)\exp(0.5q'z)$, and $F(z)=1-0.5z/D$.

271 The competing factors of $F(z)$ and $\exp(q'Z_0)$ determines the relative
 272 efficacy of epi-on and epi-off. Given the example of (at a given z), $F(z)$ of epi-on is
 273 about 0.65 of epi-off. On the other hand, the intensity reduction factor of epi-on,
 274 $\exp(-q'Z_0)=0.5$, the net gain of epi-on efficacy is $[0.65/0.5]^{0.5}=1.19$, or about 20%
 275 higher than epi-off, for the same C_0 and I_0 . However, if the epi-on RF reduction,
 276 $F(z)$, (at a given z) is lower than the gain from reduced light intensity, $\exp(q'Z_0)$,
 277 we expect a lower efficacy of epi-on. The break-even point is when $F(z)$
 278 $\exp(q'Z_0)=1$. A more rigorous analysis depends on the z -integral of $F(z)$, with $z=0$
 279 to $300 \mu\text{m}$, comparing to $\exp(q'Z_0)=1.16$ to 1.63 , for $Z_0=70$ to $100 \mu\text{m}$. We also
 280 note that three factors influencing the role of RF concentration on the CXL
 281 efficacy: the RF depletion, dynamic of light intensity, and the non-uniform
 282 distribution of RF in the stroma. The above discussed features are for the steady-
 283 state efficacy. In contrast, in the transient state (with efficacy <0.6), the efficacy
 284 is proportional to the light dose, and therefore, epi-on is always less efficient
 285 than epi-off.

286 We note that most of the currently reported epi-on efficacy is lower than
 287 that of epi-off, consistent with our transient-state efficacy. The possible factors
 288 influencing the outcomes of the reported epi-on procedure include: poor
 289 diffusion, or $F(z)<0.5$, and lack of optimal resupply of RF drops during UV

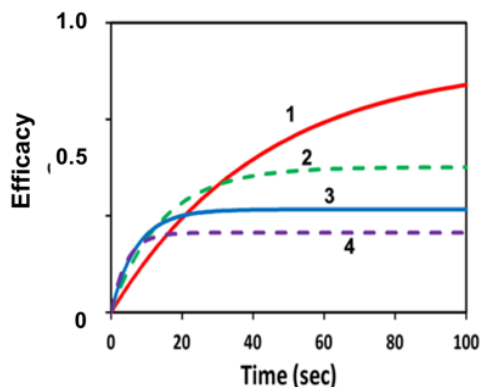
290 irradiation. Strategies for improved efficacy and crosslink depth for epi-on CXL
 291 include: the use of higher RF concentration and lower light intensity (for a given
 292 light dose); enhancing the RF diffusion by an electrode device, or diffusion
 293 enhancing medicine.

294 The comparing efficacy features of steady-state and transient state are
 295 shown in Fig. 7, based on numerical simulations [18]. Greater details for the
 296 scaling laws for steady-state and transient state efficacy (for both type-I and
 297 type-II CXL) were reported by Lin et al [18, 26]. Clinical studies of Lang et al [5]
 298 showed consistent features as our theory that accelerated CXL (ACX) had less
 299 efficacy than standard low intensity for the same fluence (dose). Moreover, most
 300 of the measured epi-on efficacy is lower than that of epi-off, consistent with our
 301 transient state prediction, but in contrary to our predicted steady-state efficacy.
 302 Therefore, further clinical studies under controlled conditions are required in
 303 order to resolve the controversial issues. My group is currently conducting CXL
 304 surgeries at Shin Kong Wu Ho-Su Memorial Hospital. A recent review comparing
 305 epi-on and epi-off was reported [31]. However, there is no direct comparing of
 306 the CXL efficacy under the same protocols.
 307



308

309 Fig. 6. Calculated CXL efficacy [15] versus corneal thickness (z) for diffusion depth
 310 $D=500 \mu\text{m}$, $C_0=0.1\%$, and for: (A) UV light intensity $I_0=10 \text{ mW/cm}^2$ for various
 311 exposure time $t=(3,5,7,10)$ sec, or dose of (0.03, 0.05, 0.07, 0.1) J/cm^2 , shown by
 312 curves (1, 2, 3, 4), respectively; and (B) for $I_0=30 \text{ mW/cm}^2$ with the same dose of (A).



313

314 Fig. 7. The calculated efficacy [18] for light intensity $I_0 = (3,9,18,30)$ mW/cm² (curves
315 1,2,3,4), and $C_0 = 0.1\%$, based on analytic formula Eq.(3).

316 **4. Conclusion**

317 Factors influencing the role of RF concentration on the CXL efficacy: the RF
318 depletion effects, dynamic of light intensity, and the non-uniform distribution of
319 RF in the stroma. The steady-state efficacy is proportional to $[F(z)C_0/I(z)]^{0.5}$, and
320 therefore epi-on is more efficient than epi-off, when the reduction factor $F(z)$
321 > 0.5 . In contrast, in the transient state (with efficacy < 0.6), the efficacy is
322 proportional to the light dose, and therefore epi-on is always less efficient than
323 epi-off. The CD has an inverse relation, such that higher light intensity and lower
324 RF concentration lead to deeper CD. The analytic formulas of Eq. (3) and (4)
325 need revisions based on numerical simulation.

326 **Acknowledgments**

327 This research is funded by the internal grants of Medical Photon, Inc.

328 **Conflicts of Interest**

329 JT Lin is the CEO of Medical Photon, Inc.
330

331 **COMPETING INTERESTS DISCLAIMER:**

332

333 **Authors have declared that no competing interests exist. The products used for**
334 **this research are commonly and predominantly use products in our area of**
335 **research and country. There is absolutely no conflict of interest between the**
336 **authors and producers of the products because we do not intend to use these**
337 **products as an avenue for any litigation but for the advancement of**
338 **knowledge. Also, the research was not funded by the producing company**
339 **rather it was funded by personal efforts of the authors.**

340 **References**

- 341 1. Hafezi F and Randleman JB. editors. Corneal Collagen Cross-linking, second ed. Thorofare (NJ): SLACK;
342 2017.
- 343 2. Spoerl E, Huhle M, Seiler T. Induction of cross-links in corneal tissue. Exp Eye Res. 1998;66:97– 103.
- 344 3. Wollensak G, Spoerl E, Seiler T. Riboflavin/ultraviolet-a-induced collagen crosslinking for the treatment of
345 keratoconus. Am J Ophthalmol. 2003;135:620–7.
- 346 4. Choi M, Kim J, Kim EK, Seo KY, Kim TI. Comparison of the conventional Dresden protocol and accelerated
347 protocol with higher ultraviolet intensity in corneal collagen cross-linking for keratoconus. Cornea.
348 2017;36(5):523– 9.
- 349 5. Lang PZ, Hafezi NL, Khandelwal SS et al. Comparative Functional Outcomes After Corneal Crosslinking
350 Using Standard, Accelerated, and Accelerated With Higher Total Fluence Protocols. Cornea 2019;38:433-
351 441.
- 352 6. Kamaev P, Friedman MD, Sherr E, Muller D. Cornea photochemical kinetics of corneal cross-linking with
353 riboflavin. Vis. Sci. 2012;53:2360-2367.
- 354 7. Schumacher S, Mrochen M, Wernli J, Bueeler M, Seiler T. Optimization model for UV-riboflavin corneal
355 cross-linking. Invest Ophthalmol Vis Sci. 2012; 53:762-769.
- 356 8. Wernli J, Schumacher S, Spoerl E, Mrochen M. The efficacy of corneal cross-linking shows a sudden
357 decrease with very high intensity UV light and short treatment time. Invest Ophthalmol Vis Sci.
358 2013;54:1176–80.
- 359 9. Semchishen A, Mrochen A, Semchishen V. Model for optimization of the UV-A/Riboflavin strengthening
360 (cross-linking) of the cornea: percolation threshold. Photochemistry and photobiology, 2015; 91:1403-
361 1411.

- 362 10. Kling S, Hafezi F. An algorithm to predict the biomechanical stiffening effect in corneal cross-linking. *J*
363 *Refract Surg* 2017; 32:128-136. doi:10.3928/1081597X-20161206-01.
- 364 11. Lin JT. Analytic formulas on factors determining the safety and efficacy in UV-light sensitized corneal
365 cross-linking. *Invest Ophthalmol Vis Sci* 2015; 56:5740-5741.
- 366 12. Lin JT. On the dynamic safety for cross linking in thin corneas (350-398 um) with extra protection under a
367 contact lens. *J Refract Sur* 2015;31,7:495-496.
- 368 13. Lin JT, Cheng DC, Chang C, Yong Zhang. The new protocol and dynamic safety of UV-light activated
369 corneal collagen cross-linking. *Chinese J Optom Ophthalmol Vis Sci.* 2015;17:140-147.
- 370 14. Lin JT. Combined analysis of safety and optimal efficacy in UV-light-activated corneal collagen
371 crosslinking. *Ophthalmology Research.* 2016; 6(2):1-14.
- 372 15. Lin JT, Cheng DC. Modelling the efficacy profiles of UV-light activated corneal collagen crosslinking. *PloS*
373 *One.* 2017;12:e0175002.
- 374 16. Lin JT. Efficacy and Z* formula for minimum corneal thickness in UV-light crosslinking. *Cornea*, 2017;
375 36:30-31.
- 376 17. Lin JT. Photochemical Kinetic modelling for oxygen-enhanced UV-light-activated corneal collagen
377 crosslinking. *Ophthalmology Research*, 2017;7:1-8.
- 378 18. Lin JT. Efficacy S-formula and kinetics of oxygen-mediated (type-II) and non-oxygen-mediated (type-I)
379 corneal cross-linking. *Ophthalmology Research.* 2018; 8(1): 1-11.
- 380 19. Lin JT. A Critical Review on the Kinetics, Efficacy, Safety, Nonlinear Law and Optimal Protocols of Corneal
381 Cross-linking. *J Ophthalmology & Visual Neuroscience*, 2018; 3:017.
- 382 20. Lin JT. A proposed concentration-controlled new protocol for optimal corneal crosslinking efficacy in the
383 anterior stroma. *Invest. Ophthalmol Vis Sci.* 2018;59:431-432.
- 384 21. Lin JT. The role of stroma riboflavin concentration in the efficacy and depth of corneal crosslinking. *Invest.*
385 *Ophthalmol Vis Sci.* 2018; 59:4449-4450.
- 386 22. Lin JT. Influencing factors relating the demarcation line depth and efficacy of corneal crosslinking. *Invest*
387 *Ophthalmol Vis Sci.* 2018;59:5125-5126.
- 388 23. Lin JT, HW Liu, Chen KT, Cheng DC. Modelling the optimal conditions for improved efficacy and crosslink
389 depth of photo-initiated polymerization. *Polymers.* 2019, 11, 217; doi:10.3390/polym11020217.
- 390 24. Lin JT. Modeling a new strategy and influencing factors for improved efficacy of accelerated corneal
391 crosslinking. *J Cataract Refract Surg*, 2019, 45, 527-529.
- 392 25. Lin JT, Chen KT, Cheng DC, Liu HW. Modeling the efficacy of radical-mediated photopolymerization: the
393 role of oxygen inhibition, viscosity and induction time. *Front. Chem.* 2019, 7:760. doi:
394 10.3389/fchem.2019.00760.
- 395 26. Lin JT. Up-dated the Critical Issues of Corneal Cross-linking (type-I and II): safety dose for ultra-thin
396 cornea, demarcation line depth and the role of oxygen. *Ophthalmology Res.* 2021;4(1);1-7.
- 397 27. Sheng SF, Lin JT. Critical analysis of corneal cross-linking(Part-I): formulas for efficacy, safety dose,
398 minimum thickness, demarcation line depth, maximum light intensity, and the role of oxygen.
399 *Ophthalmology Research, An International Journal*, 2021.14:29-41; DOI: 10.9734/OR/2021/v14i430200.
- 400 28. Hafezi F, Kling S, Gilardoni F, et al. Individualized corneal cross-linking with riboflavin and UV-A in ultra-
401 thin corneas: the sub400 protocol. *Am J Ophthalmol.* 2021;224:133-142. doi:10.1016/j.ajo.2020.12.011.
- 402 29. O'Brart NAL, O'Brart DPS, Aldahlawi et al, An Investigation of the effects of riboflavin concentration on
403 the efficacy of corneal cross-Linking using an enzymatic resistance model in porcine corneas. *Invest.*
404 *Ophthalmol Vis Sci.* 2018; 59: 1058-1065. doi:10.1167/iovs.17-22994.
- 405 30. Lombardo G, Villari V, Mical NL et al. Non-invasive Optical Method for Real-time Assessment of
406 Intracorneal Riboflavin Concentration And Efficacy Of Corneal Cross-linking. *J Biophoton*, 2018; DOI:
407 10.1002/jbio.201800028.
- 408 31. D'Oria F, Palazon A, Alio JL. Corneal collagen cross-linking epithelium-on vs. epithelium-off: a systematic
409 review and meta-analysis. *Eye and Vision* 2021 8:34.